



**NWSA-PHYSICAL SCIENCES**

Received: November 2012

Accepted: January 2013

NWSA ID : 2013.8.1.3A0062

ISSN : 1308-7304

© 2013 www.newwsa.com

**Metin Koparır**

Firat University, Elaig-Turkey

mkoparir@firat.edu.tr

**SYNTHESIS, EXPERIMENTAL AND THEORETICAL CHARACTERIZATION OF *N,N'*-DIACETYL-1,13-DIAZA-24-CROWN-8**

**ABSTRACT**

This work presents the characterization of *N,N'*-diacetyl-1,13-diaza-24-crown-8 (**I**) by quantum chemical calculations and spectral techniques. The molecular geometry and gauge including atomic orbital (GIAO) <sup>1</sup>H and <sup>13</sup>C NMR chemical shift values of **I** in the ground state have been calculated using the density functional method (B3LYP) with the 6-31G(d,p) basis set. The calculated results show that the optimized geometry can well reproduce the crystal structure, and the theoretical chemical shift values show good agreement with experimental values. The predicted non-linear optical properties of **I** are greater than ones of urea. In addition, DFT calculations of molecular electrostatic potentials and frontier molecular orbitals of **I** were carried out at the B3LYP/6-31G(d,p) level of theory.

**Keywords:** *N,N'*-diacetyl-1,13-diaza-24-crown-8, DFT, NMR, Single-Crystal X-Ray Study, MEP

***N,N'*-DİASETİL-1,13-DİAZA-24-CROWN-8'İN SENTEZİ, DENEYSEL VE TEORİK KAREKTERİZASYONU**

**ÖZET**

Bu çalışma da *N,N'*-diasetil-1,13-diaza-24-crown-8'in spektral teknikler ve kimyasal hesaplamalar ile karakterizasyonu sunulmaktadır. Molekülün geometrisi, <sup>1</sup>H ve <sup>13</sup>C kimyasal kayma değerleri yoğunluk fonksiyon metoduna (B3LYP) göre 6-31G(d,p) seti kullanılarak temel halde hesaplanmıştır. Hesaplanan optimize yapı ve kimyasal kayma değerleri deneysel sonuçlar ile iyi bir uyum içerisindedir. Molekülün doğrusal olmayan optik özellikleri üre'ye göre daha büyüktür. Bunlara ek olarak, moleküler elektrostatik potansiyel (MEP) ve sınır moleküler orbitaller B3LYP/6-31G(d,p) teori seviyesinde DFT hesaplamaları ile gerçekleştirilmiştir.

**Anahtar Kelimeler:** *N,N'*-diacetyl-1,13-diaza-24-crown-8, DFT, NMR, Single-Kristal X-Işını Çalışması, MEP

## 1. INTRODUCTION (GİRİŞ)

Synthetic macrocycles, in particular crown ethers, have been known for over three quarters of a century, although a real spate of publications in this area was observed in the late 1960s [1 and 2]. In that period, thousands of macrocyclic compounds were reported, and since then their number has increased markedly from year to year. Crown ethers contains "hard" ether-oxygen-bridges and show a binding preference toward "hard" metals (such as alkali and alkaline earth metal cation). The replacement of oxygen-bridge with "soft" sulfide or amine linkages can shift their preference towards "soft" heavy metal cations [3]. Thus, selectivity can be tuned by combining different hard/soft donor atoms in one ring system.

In recent years, density functional theory (DFT) has been extensively used in theoretical modeling. The development of better exchange-correlation functionals has made it possible to calculate many molecular properties with comparable accuracies to traditionally correlated *ab initio* methods, with more favorable computational costs [4]. Literature survey has revealed that the DFT has a great accuracy in reproducing the experimental values in geometry, dipole moment, vibrational frequency, etc. [5, 6, 7, 8 and 9].

The aim of this study is to investigate the energetic and structural properties of the crown compound, *N,N'*-diacetyl-1,13-diaza-24-crown-8 (Figure 1), using density functional theory calculations. In this study, the optimized geometry, frontier molecular orbitals (FMO), molecular electrostatic potentials (MEP) and nonlinear optical properties of **I** have been studied. These calculations are valuable for providing insight into molecular properties of crown ether compounds.

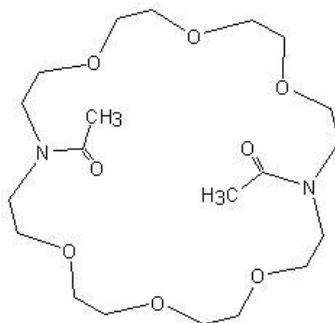


Figure 1. Chemical diagram of *N,N'*-diacetyl-1,13-diaza-24-crown-8 (Şekil. 1. *N,N'*-diacetyl-1,13-diaza-24-crown-8' in kimyasal formülü)

## 2. RESEARCH SIGNIFICANCE (ÇALIŞMANIN ÖNEMİ)

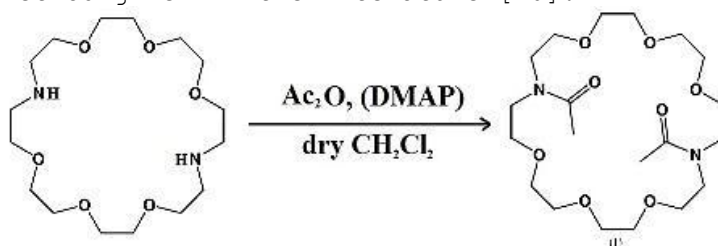
Computational chemistry and molecular modeling is a fast emerging area which is used for the modeling and simulation of small chemical and biological systems in order to understand and predict their behavior at the molecular level. It has a wide range of applications in various disciplines of engineering sciences, such as materials science, chemical engineering, biomedical engineering, etc. Knowledge of computational chemistry is essential to understand the behavior of nanosystems; it is probably the easiest route or gateway to the fast-growing discipline of nanosciences and nanotechnology, which covers many areas of research dealing with objects that are measured in nanometers and which is expected to revolutionize the industrial sector in the coming decades.

The analysis of such substances in the field of computational materials science and technology is limited, so this study has been important contribution in this field.

### 3. MATERIALS AND METHODS (MATERİYAL VE METOD)

#### 3.1. Physical Measurements and Synthesis (Fiziksel Ölçümler ve Sentez)

Melting points were determined on a Thomas Hoover melting point apparatus and uncorrected, but checked by differential scanning calorimeter (DSC). The I.R. spectra were measured with Perkin-Elmer Spectrum one FT-IR spectrophotometer. Electronic spectral studies were conducted on a Shimadzu model UV-1700 spectrophotometer in the wavelength 1100–200 nm. The  $^1\text{H}$  and  $^{13}\text{C}$  spectra were taken on Bruker AC-400 NMR spectrometer operating at 400 MHz for  $^1\text{H}$ , 100 MHz for  $^{13}\text{C}$  NMR. Compound was dissolved in  $\text{CDCl}_3$  and chemical shifts were referenced to TMS ( $^1\text{H}$  and  $^{13}\text{C}$  NMR). Starting chemicals were obtained from Merck or Aldrich. *N,N'*-diacetyl-1,13-diaza-24-crown-8 (**I**) was prepared according to a method given in the literature [10].



To a solution of 1,13-diaza-24-crown-8 (820 mg, 2.34 mmol), 4-dimethylaminopyridine (DMAP, 57 mg, 0.468 mmol) and  $\text{Et}_3\text{N}$  (824 mg, 8.1 mmol) in dry  $\text{CH}_2\text{Cl}_2$  (40 ml) was added freshly distilled  $\text{Ac}_2\text{O}$  (529 mg, 5.2 mmol), and the resulting mixture was refluxed for 2 d. The reaction mixture was allowed to cool gradually to ambient temperature and then was washed with water (3 X 50 ml). The organic layer was dried ( $\text{MgSO}_4$ ) and filtered, and the filtrate concentrated in vacuo. The residue was purified via column chromatography on silica gel by eluting with 5%  $\text{MeOH-CHCl}_3$ . Workup of the eluate afforded the title compound (280 mg, 27%) as a colorless waxy solid. Single crystals, m.p.  $85.5\pm 86.5^\circ\text{C}$ , were obtained via fractional recrystallization from  $\text{CH}_2\text{Cl}_2$ -hexane. IR (KBr) 2880 (m), 2865 (m), 1638 (s),  $1100\text{ cm}^{-1}$  (s);  $^1\text{H}$ NMR ( $\text{CDCl}_3$ )  $\delta$  2.09 (s, 6H),  $3.48\pm 3.65$  (m, 32H);  $^{13}\text{C}$  NMR ( $\text{CDCl}_3$ )  $\delta$  21.6 (q, 2C), 46.6 (t), 46.8 (t), 49.9 (t, 2C), 69.4 (t), 69.6 (t), 69.7 (t), 70.0 (t), 70.3 (t), 70.4 (t), 70.5 (t), 70.56 (t, 2C), 70.62 (t), 70.8 (t), 71.0 (t), 171.0 (t, 2C). Analysis calculated for  $\text{C}_{20}\text{H}_{38}\text{N}_2\text{O}_8$ : C 55.26, H 8.82%; found: C 55.35, H 8.76%.

#### 3.2. Computational Methods (Hesaplama Yöntemleri)

The molecular geometry was taken directly from the X-ray diffraction experimental result without any constraints. In the next step, the DFT calculations with a hybrid functional B3LYP (Becke's Three parameter hybrid functional using the LYP correlation functional) with the 6-31G(d,p) basis set using the Berny method [11 and 12] were performed with the Gaussian 09W software package [13]. To investigate the reactive sites of **I** the molecular electrostatic potentials were evaluated using B3LYP/6-31G(d,p) method. The mean linear polarizability and mean first hyperpolarizability properties of **I** were obtained from molecular polarizabilities based on theoretical calculations. In addition, frontier molecular orbitals (FMO) for the title compound were performed with B3LYP/6-31G(d,p) the optimized structure.

#### 4. FINDINGS (BULGULAR)

##### 4.1. Description of the Crystal Structure (Kristal Yapının Tanımlanması)

The crystal structure of **I** is triclinic and space group P1,  $M_w = 434.5$ ,  $a = 7.4145$  (12) Å,  $b = 8.145$  (2) Å,  $c = 10.299$  (3) Å,  $\beta = 105.103$  (18), and  $V = 550.2$  (3) Å<sup>3</sup>,  $D_x = 1.311$  g/cm<sup>3</sup>. Additional information for the structure determinations are given in Table 1. Half of the molecule makes up the asymmetric unit, the other half is generated through the crystallographic inversion center. The crown ring lies in a rough plane with the acetyl groups roughly orthogonal to that plane, but placed on opposite sides. The crown ether is collapsed in on itself, as is commonly observed in the structures of large, uncomplexed crown ethers [14].

Table 1. Crystallographic data for title compound [10].  
(Tablo 1. Başlık bileşiği için kristalografik veriler [10])

Chemical formula	C <sub>20</sub> H <sub>38</sub> N <sub>2</sub> O <sub>8</sub>
Formula weight	434.5
Temperature (K)	100
Crystal system	Triclinic
Space group	P1
Unit cell parameters	
a (Å)	7.4145 (12)
b (Å)	8.145 (2)
c (Å)	10.299 (3)
$\beta$ (°)	105.103 (18)
Volume (Å <sup>3</sup> )	550.2 (3)
Z	1
D <sub>calc</sub> (g/cm <sup>3</sup> )	1.311
Crystal size (mm)	0.52 × 0.43 × 0.30
Reflections observed [ $I > 2\sigma(I)$ ]	2357
Data/parameters	2644/137
R [ $F^2 > 2\sigma(F^2)$ ]	0.015
wR ( $F^2$ )	0.087
Goodness-of-fit on Indicator	1.03
Structure determination	SHELX97
Refinement	Full matrix
$\Delta\rho_{max}, \Delta\rho_{min}$ (e/Å <sup>3</sup> )	0.34, -0.23

This is the first X-ray structure of a 24-crown-8 ether without sterically constraining groups on the crown backbone (such as benzo or cyclohexano). As such, it may represent a relatively low energy conformation for 24-crown-8. The collapse of an uncomplexed crown ring typically leads to favorable intramolecular C-H...O bonding [19], which may influence the observed conformation. Only one such bond is observed here (C1-H1B...O3), but an intramolecular H bond is also observed between one of the acetyl methyl H atoms and O1 (Table 2). The orientation of the acetyl group may also be affected by a short contact between O4 and H8B (2.42 Å, see Table 2).

Table 2. Hydrogen bonding geometry ( $\text{\AA},^\circ$ ) for the title compound.

(Tablo 2. Başlık bileşiği için hidrjen bağı geometrisi ( $\text{\AA},^\circ$ ))

D - H...A	D - H	H...A	D...A	D - H...A
C1 - H1B...O3	0.99	2.49	3.1181 (15)	121
C2 - H2A...O4 <sup>i</sup>	0.99	2.52	3.4804 (16)	163
C6 - H6A...O2 <sup>ii</sup>	0.99	2.58	3.5592 (16)	169
C8 - H8A...O4	0.99	2.42	2.6822 (15)	94
C10 - H10B...O1	0.98	2.42	3.2613 (16)	144

Symmetry code: (i) - x, 1 - y, 1 - z ; (ii) x, y, 1 + z.

#### 4.2. Optimized Geometry (Geometrinin Optimizasyonu)

The optimized parameters (bond lengths, bond angles, and dihedral angles) of **I** were obtained using the B3LYP/6-31G(d,p) method. The atomic numbering scheme of the theoretical geometric structure is shown in Fig. 2B. Calculated geometric parameters are listed in Table 3 along with the experimental data. When the X-ray structure of **I** is compared with its optimized counterparts (see Figure 3), slight conformational discrepancies are observed between them. We note that the experimental results are for the solid phase and the theoretical calculations are for the gas phase. In the solid state, the existence of a crystal field along with the intermolecular interactions connects the molecules together, which results in the differences in bond parameters between the calculated and experimental values.

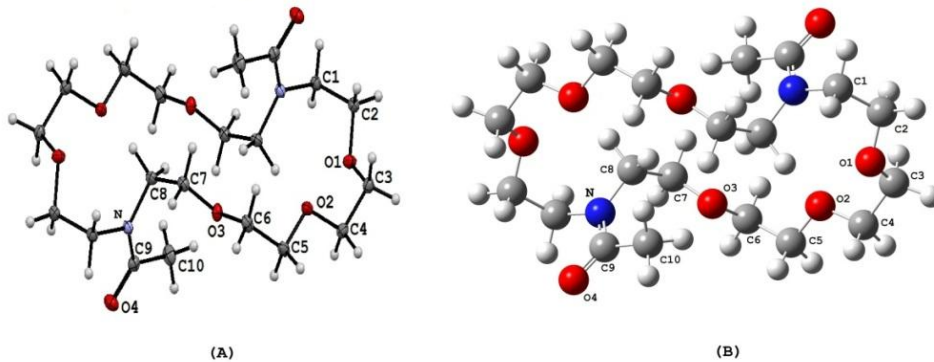


Figure 2. (A) Ortep-3 diagram of the title compound (B) The theoretical geometric structure of the title compound (with B3LYP/6-31G(d,p) level).

(Şekil 2. (A) Başlık bileşiğinin Ortep-3 yapısı (B) Başlık bileşiğinin hesaplanan geometrik yapısı (B3LYP/6-31G(d,p) seviyesi ile).

Table 3. Selected molecular structure parameters.  
 (Tablo 3. Seçilmiş moleküler yapı parametreleri)

Parameters	Experimental	B3LYP/6-31G(d,p)
<b>Bond lengths (Å)</b>		
O(1)-C(2)	1.4297 (13)	1.4228
O(1)-C(3)	1.4218 (11)	1.4176
O(2)-C(4)	1.4209 (13)	1.4146
O(2)-C(5)	1.4292 (14)	1.4171
O(3)-C(6)	1.4268 (12)	1.4134
O(3)-C(7)	1.4202 (12)	1.4215
O(4)-C(9)	1.2342 (12)	1.2308
N-C(1)	1.4666 (13)	1.4655
N-C(8)	1.4642 (14)	1.4638
N-C(9)	1.3511 (14)	1.3754
RMSE <sup>a</sup>		0.013
<b>Bond Angles (°)</b>		
C(2)-O(1)-C(3)	112.18 (8)	113.03
C(4)-O(2)-C(5)	111.43 (7)	113.05
C(6)-O(3)-C(7)	115.90 (7)	115.86
C(1)-N-C(8)	116.92 (8)	117.25
C(1)-N-C(9)	125.10 (9)	125.14
C(8)-N-C(9)	117.65 (8)	116.82
N-C(1)-C(2)	112.65 (8)	114.07
O(1)-C(2)-C(1)	108.27 (8)	110.04
O(1)-C(3)-C(4)	109.16 (8)	110.10
O(2)-C(4)-C(3)	109.46 (8)	109.59
O(2)-C(5)-C(6)	108.89 (8)	109.12
O(3)-C(6)-C(5)	109.48 (7)	109.09
O(3)-C(7)-C(8)	108.01 (8)	108.41
N-C(8)-C(7)	110.81 (8)	112.03
O(4)-C(9)-N	121.24 (10)	120.98
O(4)-C(9)-C(10)	120.40 (10)	121.24
N-C(9)-C(10)	118.36 (9)	117.78
RMSE <sup>a</sup>		0.489
<b>Dihedral angles (°)</b>		
C(3)-O(1)-C(2)-C(1)	175.08 (8)	169.60
C(2)-O(1)-C(3)-C(4)	174.85 (8)	174.02
C(5)-O(2)-C(4)-C(3)	-178.31 (7)	-176.92
C(4)-O(2)-C(5)-C(6)	173.89 (7)	175.87
C(7)-O(3)-C(6)-C(5)	143.41 (9)	154.89
C(6)-O(3)-C(7)-C(8)	-148.26 (9)	-151.92
C(1)-N-C(8)-C(7)	-93.00 (9)	-90.74
C(8)-N-C(1)-C(2)	-87.04 (10)	-91.53

<sup>a</sup> Between the bond lengths and the bond angles computed by the theoretical method and those obtained from X-ray diffraction.

A logical method for globally comparing the structures obtained with the theoretical calculations is by superimposing the molecular skeleton with that obtained from X-ray diffraction, giving a RMSE of 0.137 Å for B3LYP/6-31G(d,p) (Figure 3). This magnitude of RMSE can be explained by the fact that the intermolecular Coulombic interaction with the neighboring molecules are absent in gas phase, whereas the experimental result corresponds to interacting molecules in the crystal lattice [16].

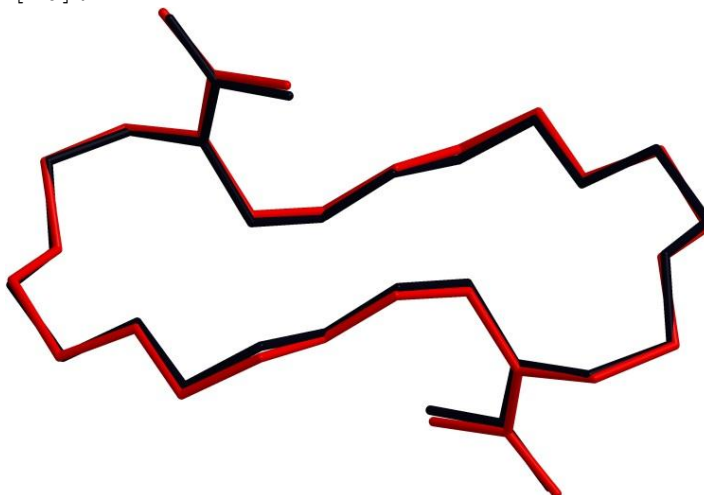


Figure 3. Atom-by-atom superimposition of the structures calculated (red) over the X-ray structure (black) for the title compound.

(Şekil 3. Hesaplanan yapı (kırmızı) ve X-ışını yapısının (siyah) üst üste çakıştırılması)

#### 4.3. NMR Spectra (NMR Spektrumu)

GIAO  $^1\text{H}$  and  $^{13}\text{C}$  chemical shift values (with respect to TMS) were calculated using the B3LYP method with 6-31G(d,p) basis set and generally compared to the experimental  $^1\text{H}$  and  $^{13}\text{C}$  chemical shift values. The results of this calculation are shown in Table 4.

We have calculated  $^1\text{H}$  chemical shift values (with respect to TMS) of 2.60-4.24 ppm at B3LYP/6-31G(d,p) level, whereas the experimental results are observed to be 2.09-3.65 ppm. The singlet observed at 2.09 ppm is assigned to C(10)H<sub>2</sub> and multiplet observed at 3.48-3.65 ppm is assigned to C(1)H<sub>2</sub>-C(8)H<sub>2</sub> that have been calculated at 2.60 and 3.60-4.24 ppm.

We have calculated  $^{13}\text{C}$  chemical shift values (with respect to TMS) of 30.97-162.02 ppm with B3LYP/6-31G(d,p), while, the experimental results were observed to be 46.6-171.0 ppm. As can be seen from Table 4, theoretical  $^1\text{H}$  and  $^{13}\text{C}$  chemical shift results of the title compound are generally closer to the experimental chemical shift data.

Table 4. Theoretical and experimental  $^1\text{H}$  and  $^{13}\text{C}$  isotropic chemical shifts for the title compound.

(Tablo 4. Başlık bileşiği için  $^1\text{H}$  ve  $^{13}\text{C}$  kimyasal kayma değerleri)

Atom	Experimental (ppm) ( $\text{CDCl}_3$ )	Calculated (ppm) B3LYP/6-31G(d,p)
C1	49.9	50.67
C2	70.62	71.15
C3	70.0	70.32
C4	69.4	69.7
C5	69.9	69.93
C6	71.0	71.37
C7	70.03	70.42
C8	46.66	46.37
C9	171.0	162.02
C10	21.6	30.97
2H (C(1)H <sub>2</sub> )	3.60	4.04
2H (C(2)H <sub>2</sub> )	3.65	4.10
2H (C(3)H <sub>2</sub> )	3.45	3.94
2H (C(4)H <sub>2</sub> )	3.63	4.22
2H (C(5)H <sub>2</sub> )	3.49	3.6
2H (C(6)H <sub>2</sub> )	3.60	4.23
2H (C(7)H <sub>2</sub> )	3.56	4.15
2H (C(8)H <sub>2</sub> )	3.62	4.24
3H (C(10)H <sub>3</sub> )	2.09	2.6

#### 4.4. Molecular Electrostatic Potential (Moleküler Elektrostatik Potansiyel)

Molecular electrostatic used extensively for interpreting potentials have been and predicting the reactive behavior of a wide variety of chemical system in both electrophilic and nucleophilic reactions, the study of biological recognition processes and hydrogen bonding interactions [17].

$V(\mathbf{r})$ , at a given point  $\mathbf{r}(x, y, z)$  in the vicinity of a molecule, is defined in terms of the interaction energy between the electrical charge generated from the molecule electrons and nuclei and positive test charge (a proton) located at  $\mathbf{r}$ . Unlike many of the other quantities used at present and earlier as indices of reactivity,  $V(\mathbf{r})$  is a real physical property that can be determined experimentally by diffraction or by computational methods. For the systems studied the MEP values were calculated as described previously, using the equation [18]:

$$V(\mathbf{r}) = \sum \frac{Z_A}{|\mathbf{R}_A - \mathbf{r}|} - \int \frac{\rho(\mathbf{r}')}{|\mathbf{r}' - \mathbf{r}|} d\mathbf{r}'$$

where the summation runs over all the nuclei  $\mathbf{A}$  in the molecule and polarization and reorganization effects are neglected.  $Z_A$  is the charge of the nucleus  $\mathbf{A}$ , located at  $\mathbf{R}_A$  and  $\rho(\mathbf{r}')$  is the electron density function of the molecule. To predict reactive sites for electrophilic and nucleophilic attack for the investigated molecule, molecular electrostatic potential (MEP) was calculated at

B3LYP/6-31G(d,p) optimized geometries. Red and blue areas in the MEP map refer to the regions of negative and positive potentials and correspond to the electron-rich and electron-poor regions, respectively, whereas the green color signifies the neutral electrostatic potential. The MEP surface provides necessary information about the reactive sites.

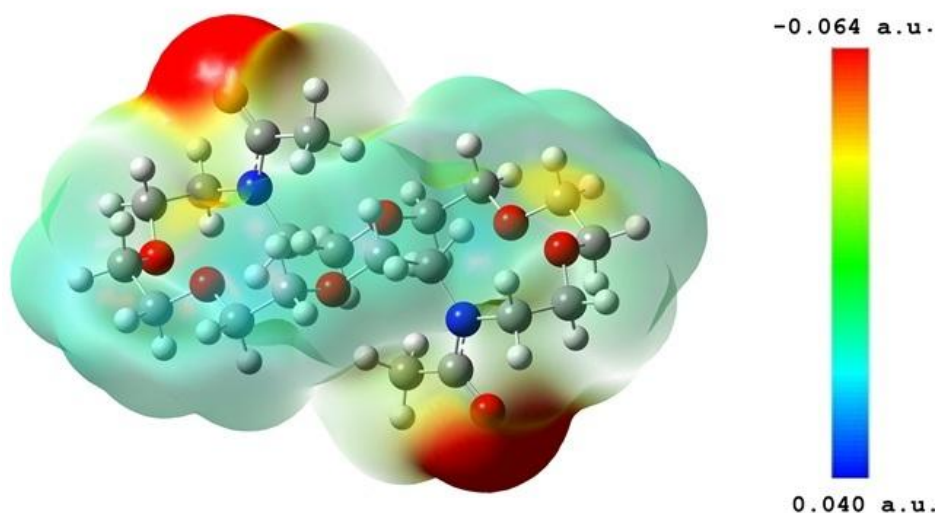


Figure 4. Molecular electrostatic potential map calculated at B3LYP/6-31G(d,p) level.  
(Şekil 4. B3LYP/6-31g(d,p) seviyesinde yapının moleküler elektrostatik haritası.)

The negative regions  $V(\mathbf{r})$  were related to electrophilic reactivity and the positive ones to nucleophilic reactivity. As easily can be seen in Figure 4, this molecule has several possible sites for electrophilic attack in which  $V(\mathbf{r})$  calculations have provided insights. Negative regions in the studied molecule were found around the O4 atom and N atom. The negative  $V(\mathbf{r})$  values are -0.064 a.u. for O4 atom, which is the most negative region, -0.038 a.u. for N atom which is a less negative region. According to these calculated results, the MEP map shows that the negative potential sites are on electronegative atoms as well as the positive potential sites are around the hydrogen atoms. These sites give information about the region from where the compound can have intermolecular interactions.

#### 4.5. Frontier Molecular Orbitals (Sınır Moleküler Orbitaler)

In principle, there are several ways to calculate the excitation energies. The simplest one involves the difference between the highest occupied molecular orbital (HOMO) and the lowest unoccupied molecular orbital (LUMO) of a neutral system, which is a key parameter in determining molecular properties [19]. Moreover, the Eigen values of HOMO ( $\pi$  donor) and LUMO ( $\pi$  acceptor) and their energy gap reflect the chemical activity of the molecules. Recently, the energy gap between HOMO and LUMO has been used to prove the bioactivity from intramolecular charge transfer (ICT) [20 and 21]. Figure 5 shows the distributions and energy levels of the HOMO-1, HOMO, LUMO and LUMO+1 orbitals computed at the B3LYP/6-31G(d,p) level for **I**. As seen from Figure 5, both in the HOMO and HOMO-1, electrons are delocalized on the O4 atom and N atom. For the LUMO and LUMO+1 electrons are mainly delocalized on the N, C9, C10 and O4 atoms. The value of the energy

separation between the HOMO and LUMO is 7.124 eV. This large HOMO-LUMO gap automatically means high excitation energies for many of excited states, a good stability and a high chemical hardness for **I**.

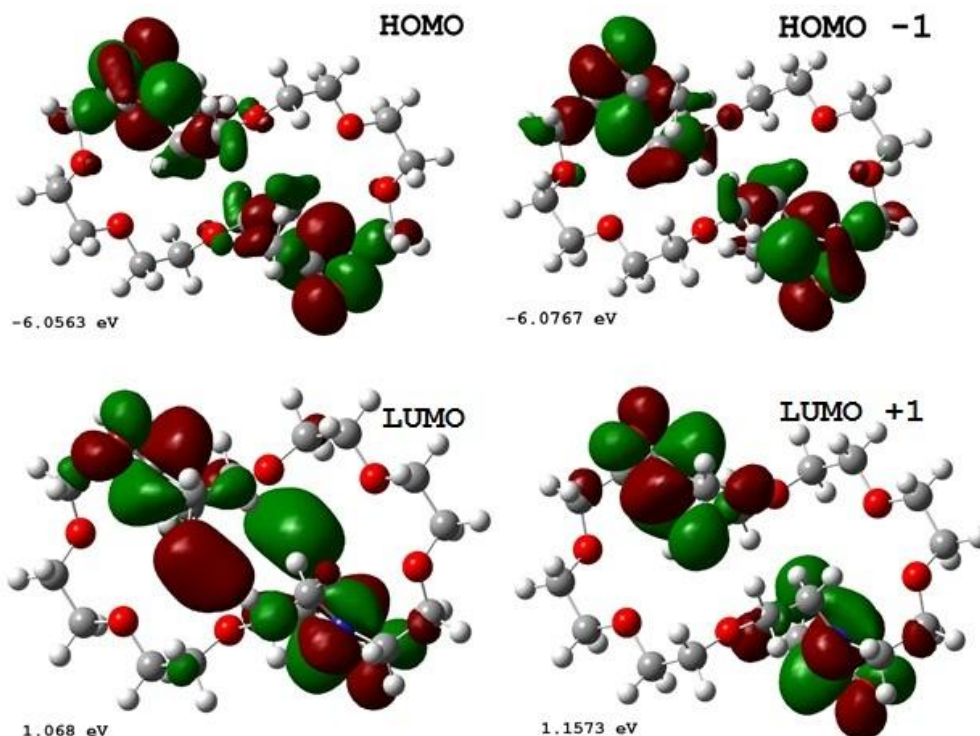


Figure 5. Molecular orbital surfaces and energy levels given for the HOMO, HOMO -1, LUMO and LUMO + 1 of the title compound computed at B3LYP/6-31G(d,p) level

(Şekil 5. Başlık bileşiğinin B3LYP/6-31G(d,p) seviyesinde hesaplanan HOMO, HOMO -1, LUMO ve LUMO + 1 moleküler orbitalleri ve enerji düzeyleri)

#### 4.6. Nonlinear Optical Effects (Doğrusal Olmayan Optik Etkileri)

NLO properties has been of great interest by the recent years. Because some synthesized novel materials show efficient nonlinear optical that are used telecommunication, potential applications in modern communication technology, optical signal processing and data storage.

The calculations of the total molecular dipole moment ( $\mu$ ), linear polarizability ( $\alpha$ ) and first-order hyperpolarizability ( $\beta$ ) from the Gaussian output have been explained in detail previously [22], and DFT has been extensively used as an effective method to investigate the organic NLO materials. It is well known that from the literature, the B3LYP approach provides fairly reliable values in electric hyperpolarizability calculations when compared with accuracies of traditional *ab initio* methods and this predictive capability of widely used B3LYP method is of interest to a wide audience of computational scientists [23,24]. In addition, taking into account reliability and the computational time required [25], the basis set 6-31G(d,p) was chosen for the calculations of the hyperpolarizability in this study.

The electronic dipole moment  $\mu_i$  ( $i = x, y, z$ ), polarizability  $\alpha_{ij}$  and the first hyperpolarizability  $\beta_{ijk}$  of **I** were calculated at the B3LYP/6-31G(d,p) level using Gaussian 09W program package. Urea is one of the prototypical molecules used in the study of the NLO properties

of molecular systems. Therefore it was used frequently as a threshold value for comparative purposes. The calculated values of  $\alpha_{\text{tot}}$  and  $\beta_{\text{tot}}$  for **I** are, 37.849 Å<sup>3</sup> and  $2.727 \times 10^{-30}$  cm<sup>5</sup>/esu, which are greater than those of urea (the  $\alpha_{\text{tot}}$  and  $\beta_{\text{tot}}$  of urea are 3.831 Å<sup>3</sup> and  $0.37 \times 10^{-30}$  cm<sup>5</sup>/esu obtained by B3LYP/6-31G(d,p) method). According to the magnitude of the first hyperpolarizability, **I** may be a potential applicant in the development of NLO materials.

## 5. CONCLUSIONS (SONUÇLAR)

The investigation of the present work is illuminate the spectroscopic properties such as molecular parameters and magnetic properties of title compound by using <sup>1</sup>H and <sup>13</sup>C NMR techniques and tools derived from the density functional theory. Due to the lack of experimental information on the structural parameters available in the literature, the optimized geometric parameters (bond lengths and bond angles) was theoretically determined at B3LYP/6-31G(d,p) level of theory and compared with the structurally similar compounds. The X-ray structure is found to be very slightly different from its optimized counterpart. It was noted here that the experimental results belong to solid phase and theoretical calculations belong to gaseous phase. In the solid state, the existence of the crystal field along with the intermolecular interactions have connected the molecules together, which result in the differences of bond parameters between the calculated and experimental values. Despite the differences observed in the geometric parameters, the general agreement is good and the theoretical calculations support the solid-state structure. The magnetic properties of the title molecule were observed and calculated the same method. The chemical shifts were compared with experimental data in CDCl<sub>3</sub> solution, showing a very good agreement both for <sup>13</sup>C and <sup>1</sup>H chemical shifts. When all theoretical results scanned, they are showing good correlation with experimental data.

## REFERENCES (KAYNAKLAR)

1. Melson, G.A., (1979). Coordination Chemistry of Macrocyclic Compounds. New York: Plenum Publishing Corp.
2. Formanowskii, A.A. and Mikhura, I.V., (1997). Synthesis of Macrocyclic Compounds. In Macrocyclic Compounds in Analytical Chemistry. New York: Wiley- Interscience.
3. Chartres, J.D., Davies, M.S., Lindoy, L.F., Meehan, G.V., and Wei, G., (2006). Macrocyclic Ligand Design: The Interaction of Selected Transition and Post-Transition Metal Ions With a 14-Membered N2S2-Donor Macrocycle. Inorganic Chemistry Communications, Volume:2006, pp.:751-754.
4. Proft, F.D. and Geerlings, P., (2001). Conceptual and computational DFT in the study of aromaticity. Chemical Reviews, Volume:101, pp.:1451-1464.
5. Orek, C., Koparır, P., and Koparır, M., (2012). N-Cyclohexyl-2-[5-(4-pyridyl)-4-(p-tolyl)-4H-1,2,4-triazol-3-ylsulfanyl]-acetamide dihydrate: Synthesis, experimental, theoretical characterization and biological activities. Spectrochimica Acta Part A: Molecular and Biomolecular Spectroscopy, Volume:97, pp.:923-934.
6. Cansız, A., Cetin, A., Orek, C., Karatep, M., Sarac, K., Kus, A., and Koparır, P., (2012). 6-Phenyl-3-(4-pyridyl)-1,2,4-triazolo-[3,4-b][1,3,4]thiadiazole: Synthesis, experimental, theoretical characterization and biological activities. Spectrochimica Acta Part A: Molecular and Biomolecular Spectroscopy, Volume:97, pp.:607-615.



7. Tanak, H., (2011). DFT computational modeling studies on 4-(2,3-Dihydroxybenzylideneamino)-3-methyl-1H-1,2,4-triazol-5(4H)-one. *Computational And Theoretical Chemistry*, Volume:967, pp: 93-101
8. Andzelm, J. and Fitzgerald, G., (1991). Chemical Applications of Density Functional Theory - Comparison to Experiment, Hartree-Fock, and Perturbation-Theory. *Journal of Physical Chemistry*, Volume:95, pp:10531-10534
9. Andzelm, J. and Wimmer, E., (1992). Density Functional Gaussian-Type-Orbital Approach to Molecular Geometries, Vibrations, and Reaction Energies. *Journal of Chemical Physics*, Volume:96, pp:1280-1303
10. Jeffrey, C.B., Alan, P.M., and Hazlewood, A., (2000). N,N'-Diacetyl-1,13-diaza-24-crown-8. *Acta Crystallographica Section E Structure Reports Online*, Volume:E57, pp.:13-15.
11. Schlegel, H.B., (1982). Optimization of Equilibrium Geometries and Transition Structure. *Journal of Computational Chemistry*, Volume:3, pp:214-218
12. Peng, C., Ayala, P.Y., and Schlegel, H.B., (1996). Using Redundant Internal Coordinates to Optimize Equilibrium Geometries and Transition States. *Journal of Computational Chemistry*, Volume:17, pp:49-56
13. M.J. Frisch, G.W. Trucks, H.B. Schlegel, G.E. Scuseria, M.A. Robb, J.R. Cheeseman, G. Scalmani, V. Barone, B. Mennucci, G.A. Petersson, H. Nakatsuji, M. Caricato, X. Li, H.P. Hratchian, A.F. Izmaylov, J. Bloino, G. Zheng, J.L. Sonnenberg, M. Hada, M. Ehara, K. Toyota, R. Fukuda, J. Hasegawa, M. Ishida, T. Nakajima, Y. Honda, O. Kitao, H. Nakai, T. Vreven, J.A. Montgomery, Jr., J.E. Peralta, F. Ogliaro, M. Bearpark, J.J. Heyd, E. Brothers, K.N. Kudin, V.N. Staroverov, R. Kobayashi, J. Normand, K. Raghavachari, A. Rendell, J.C. Burant, S.S. Iyengar, J. Tomasi, M. Cossi, N. Rega, J.M. Millam, M. Klene, J.E. Knox, J.B. Cross, V. Bakken, C. Adamo, J. Jaramillo, R. Gomperts, R.E. Stratmann, O. Yazyev, A.J. Austin, R. Cammi, C. Pomelli, J.W. Ochterski, R.L. Martin, K. Morokuma, V.G. Zakrzewski, G.A. Voth, P. Salvador, J.J. Dannenberg, S. Dapprich, A.D. Daniels, O. Farkas, J.B. Foresman, J.V. Ortiz, J. Cioslowski, and D.J. Fox, Gaussian, Inc., Wallingford CT, 2009.
14. Bryan, J.C., Lavis, J.M., Hay, B.P., and Sachleben, R.A., (2000). N-ethylazatribenzo-21-crown-7. *Acta Crystallographica Section C-Crystal Structure Communications*, Volume:56, pp.:391-392.
15. Bryan, J.C., Bunick, G.J., and Sachleben, R.A., (1999). Tetrabenzo-24-crown-8. *Acta Crystallographica Section C-Crystal Structure Communications*, Volume:55, pp.:250-252.
16. Tanak, H., (2011). Crystal Structure, Spectroscopy, and Quantum Chemical Studies of  $\epsilon$ -2[(2-Chlorophenyl)iminomethyl]-4-trifluoromethoxyphenol. *Journal of Physical Chemistry A*, Volume:115, pp.:13865-13876
17. Politzer, P. and Murray, J.S., (1991). *Theoretical biochemistry and molecular biophysics: a comprehensive survey*. Adenine Press, Schenectady, NY.
18. Politzer, P. and Murray, J.S., (2002). *The Fundamental Nature and Role of the Electrostatic Potential in Atoms and Molecules*. *Theoretical Chemistry Accounts*, Volume:108, pp.: 134.
19. Amalanathan, M., Rastogi, V.K., Joe, I.H., Palafox, M.A., and Tomar, R., (2009). Density functional theory calculations and vibrational spectral analysis of 3,5-(dinitrobenzoic acid).



- Spevtrichimica Acta Part A-Molecular and Biomolecular Spectroscopy, Volume:78, pp.:1437-1444.
20. Padmaja, L., Ravikumar, C., Sajan, D., Joe, I.H., Jayakumar, V.S., Pettit, G.R., and Nielsen, O.F., (2009). Density Functional Study on the Structural Conformations and Intramolecular Charge transfer From the Vibrational Spectra of the Anticancer Drug Combretastatin. *Journal of Raman Spectroscopy*, Volume:40, pp.:419-428.
  21. Sagdinc, S. and Pir, H., (2009). Spectroscopic and DFT studies of flurbiprofen as dimer and its Cu(II) and Hg(II) complexes. *Spectrochimica Acta Part A-Molecular and Biomolecular Spectroscopy*, Volume:73, pp.:181-187.
  22. Thanthiriwatte, K.S. and de Silva, K.M.N., (2002). Non-linear Optical Properties of Novel Fluorenyl Derivatives - ab Initio Quantum Chemical Calculations. *Journal of Molecular Structure-Theochem*, Volume:617, pp.:169-175.
  23. Maroulis, G., Begue, D., and Pouchan, C., (2003). Accurate Dipole Polarizabilities of Small Silicon Clusters From ab Initio and Density Functional Theory Calculations. *Journall of Chemical Physics*, Volume:119, pp.:794-798.
  24. Maroulis, G., (2008). How Large is the Static Electric (hyper)Polarizability Anisotropy in HXeI. *Journal of Chemical Physics*, Volume:129, pp.:044314-044321.
  25. Qin, C., Si, Y., Yang, G., and Su, Z., (2011). Quantum Chemical Study of Structures, Electronic Spectrum, and Nonlinear Optical Properties of Polynuclear Lithium Compounds. *Computational and Theoretical Chemistry*, Volume:966, pp.: 14-19.